The landing problem of a VTOL Unmanned Aerial Vehicle on a moving platform using optical flow

Bruno Herisse, Tarek Hamel, Robert Mahony, Francois-Xavier Russotto

***Abstract*— This paper presents a nonlinear controller for hovering flight and landing control on a moving platform for a Vertical Take-off and Landing (VTOL) Unmanned Aerial Vehicle (UAV) by exploiting the measurement of the average optical flow. The VTOL vehicle is assumed to be equipped with a minimum sensor suite (a camera and an IMU), manoeuvring over a textured flat target plane. Two different tasks are considered in this paper: the first one concerns the stability of hovering flight and the second one concerns regulation of automatic vertical landing on a moving platform using the divergent optical flow as feedback information. Simulation and experimental results performed on a quad-rotor UAV demonstrate the performance of the proposed control strategy.**

I. INTRODUCTION

Recent advances in technology and potential applications have led to a growing interest in aerial robotic [25]. UAVs turn out to be necessary for many indoor and outdoor applications that jeopardize human or material safety such as military or civilian inspection, hazardous material transportation, navigation through cluttered environments and close to obstructions (obstacle avoidance, take-off and landing), etc. A major issue in UAV control is the difficulty of landing the vehicle on a moving platform such as a ship deck or a landing pad, a field that has been investigated using a prediction or a model of the vertical motion of landing platform [16], [26], a tether-guide [18] or a known target [22], [21]. The main idea of the prior work consists in obtaining a knowledge of the motion of the platform to perform a landing manoeuvre that ensures the safety of the vehicle as well as possible by providing a feed-forward compensation. An alternative approach that stems from the insight into the behaviour of flying insects and animals uses visual flow [23]. Since optical flow provides relative velocity and proximity informations with respect to obstacles [12], it is an ideal cue that can be used to perform landing control strategies [23], [19] as well as obstacle avoidance [2], [7], [4], terrain following [10], [20], [6] or even visual servo control [14]. It is rare that mobile obstacles are considered in such robotic applications using optical flow but it is well known that insects show great capabilities in achieving landing tasks on a moving object such as, for example, a bee landing on a flower. Moreover, the full vehicle dynamics analysis is rarely discussed. the flight regime of insects is highly damped due to their high drag to mass ratios and the control strategies that have been observed in the various biological studies do not generalise to high-inertia, low-drag aerial vehicles.

In this paper, a control law for hovering flight and landing manoeuvre on a moving platform of a UAV capable of quasi stationary flight is proposed by focusing just on the translational dynamics of the vehicle. A 'high gain' controller is used to stabilise the orientation dynamics, an approach classically known in aeronautics as guidance and control (or hierarchical control) [3]. The image feature considered is the average optical flow obtained from the measurement of the optical flow of a textured target plane in the inertial frame using additional information provided by an embedded IMU for *derotation* of the flow. A non-linear PI-type controller is designed for hovering flight while another nonlinear controller, exploiting the vertical optical flow (similar to the optical flow divergence) as feedback information, is proposed for vertical landing on a moving platform with bounded dynamics. Lyapunov analysis is used to prove semi-global exponential stability and convergence of the closed-loop system for the considered objectives. Experimental results are obtained on a quad-rotor UAV capable of quasi-stationary flight developed at CEA (French Atomic Energy Commission). The proposed closed-loop control schemes demonstrate efficiency and performance for the hovering flight and vertical landing manoeuvre.

The body of the paper consists of five sections followed by a conclusion. Section II presents the fundamental equations of motion for an X4-flyer UAV. Section III describes the average optical flow that is used and presents the control strategy for hovering manoeuvre. Section IV presents the proposed control strategy and the stability analysis adopted for the vertical landing manoeuvre. Section V describes simulations results and finally Section VI describes the experimental results obtained on the quad-rotor vehicle.

II. UAV DYNAMIC MODEL AND TIME SCALE SEPARATION

The VTOL UAV is represented by a rigid body, of mass m and of tensor of inertia $\mathbf{I}$, with external forces due to gravity and forces and torques applied by rotors. To describe the motion of the UAV, two reference frames are introduced: an inertial reference frame $\mathcal{I}$ associated with the vector basis $[e_1, e_2, e_3]$ and a body-fixed frame $\mathcal{B}$ attached to the UAV at the center of mass and associated with the vector basis $[e_1^b, e_2^b, e_3^b]$. The position and the linear velocity of the UAV in $\mathcal{I}$ are respectively denoted $\xi = (x, y, z)^T$ and $v = (\dot{x}, \dot{y}, \dot{z})^T$. The orientation of the UAV is given by the orientation matrix

B. Herisse and F.-X. Russotto are with CEA, LIST, Interactive Robotics Laboratory, Fontenay aux Roses, F-92265, France firstname.lastname@cea.fr

T. Hamel is with I3S, UNSA - CNRS, Sophia Antipolis, France thamel@i3s.unice.fr

R. Mahony is with Dep. of Eng., Australian Nat. Univ., Canberra ACT, 0200, Australia Robert.Mahony@anu.edu.au

$R \in SO(3)$ from $\mathcal{B}$ to $\mathcal{I}$. Finally, let $\Omega = (\Omega_1, \Omega_2, \Omega_3)^T$ be the angular velocity of the UAV defined in $\mathcal{B}$.

A translational force F and a control torque Γ are applied to the UAV. The translational force F combines thrust, lift, drag and gravity components. For a miniature VTOL UAV in quasi-stationary flight one can reasonably assume that the aerodynamic forces are always in direction e_3^b, since the thrust force predominates over other components [15]. The gravitational force can be separated from other forces and the dynamics of the VTOL UAV can be written as:

$$\dot{\xi} = v \tag{1}$$
$$m\dot{v} = -TRe_3 + mge_3 + \Delta \tag{2}$$
$$\dot{R} = R\Omega_\times, \tag{3}$$
$$\mathbf{I}\dot{\Omega} = -\Omega \times \mathbf{I}\Omega + \Gamma, \tag{4}$$

In the above notation, g is the acceleration due to gravity, and T a scalar input termed the thrust or heave, applied in direction $e_3^b = Re_3$ where e_3 is the third-axis unit vector $(0, 0, 1)$. The term Δ gathers all disturbances and unknown dynamics. The matrix $\Omega_\times$ denotes the skew-symmetric matrix associated to the vector product $\Omega_\times x := \Omega \times x$ for any x.

The full vectorial term TRe_3 will be considered as control input for the translational dynamics (2). We will assign its desired value $u \equiv (TRe_3)^d = T^d R^d e_3$. Assuming that actuator dynamics can be neglected, the value T^d is considered to be instantaneously reached by T. For the orientation dynamics of (3)-(4), a high gain controller is used to ensure that the orientation R of the UAV converges to the desired orientation R^d. The resulting control problem is then simplified to

$$\dot{\xi} = v,\ m\dot{v} = -u + mge_3 + \Delta \tag{5}$$

Thus, we consider only the control of the translational dynamics (5) with a direct control input u. This common approach is used in practice and may be justified theoretically using singular perturbation theory [11].

III. Stabilisation of the Hovering flight

In this section a control design ensuring hovering flight over a static textured flat plane is proposed. The camera is assumed to be attached to the center of mass so that the focal point of the camera coincides with the origin of the body-fixed frame. The control problem considered is the stabilisation of the linear velocity about zero despite unmodeled constant (or slowly time varying) dynamics by exploiting the measurement of the average optical flow[1]. Note that due to the rotational ego-motion of the camera, the optical flow involves the angular velocity as well as the linear velocity [12]. Let $\eta \in \mathcal{I}$ denote the unit normal to the target plane. We define an inertial average optical flow from the integral of all observed optical flow around the direction of observation η corrected for rotational angular velocity

$$w = -(R_t \Lambda^{-1} R_t^T) R \iint_{\mathcal{W}^2} (\dot{p} + \Omega \times p)\ dp \tag{6}$$

where $\dot{p}$ is the derivative of an image point p observed by a spherical camera, $\mathcal{W}^2$ is the aperture around η, Λ is a diagonal matrix depending on the aperture and R_t is the orientation matrix from a frame of reference with η in the z-axis to the inertial frame $\mathcal{I}$ (see details in [9]). The orthogonal distance of the camera to that target plane is denoted $d = -\langle \xi, \eta \rangle$. One has that

$$w = \frac{v}{d} + noise \tag{7}$$

In this section, A PI-type non-linear controller depending only on the measurable variable w is proposed for the translational dynamics (5). The result is stated in the following theorem.

Theorem 3.1: Assume that η is known and invariant and Δ is a constant. Consider the dynamics (5) and assume that the control input u is chosen as

$$u = k_P w + k_I \int_0^t w d\tau + mge_3,\ \ k_P, k_I > 0 \tag{8}$$

Then, for any initial conditions $d_0 = d(0) > 0$, the linear velocity v converges asymptotically towards zero. More precisely:

1) $\dot{d} = -\langle v, \eta \rangle$ converges to 0 while guarantying that $d(t) = -\langle \xi, \eta \rangle > 0,\ \forall t$,
2) the horizontal velocity $v^{\parallel} = \pi_\eta v$ converges to zero.

Proof:

Proof of part 1: Recall the dynamics of the vehicle (5) and consider the component $v^\perp = \langle v, \eta \rangle$ in direction η, it yields:

$$m\dot{v}^\perp = -k_P \frac{v^\perp}{d} - k_I \int_0^t \frac{v^\perp}{d} d\tau + \langle \Delta, \eta \rangle \tag{9}$$

Note that $v^\perp = -\dot{d}$. Equation (9) can also be written as follows:

$$m\ddot{d} = -k_P \frac{\dot{d}}{d} - k_I \int_0^t \frac{\dot{d}}{d} d\tau - \langle \Delta, \eta \rangle \tag{10}$$
$$= -k_P \frac{\dot{d}}{d} - k_I \ln\left(\frac{d}{d_\infty}\right) \tag{11}$$

where $d_\infty = d_0 e^{-\langle \Delta, \eta \rangle / k_I}$. The control law is well defined and smooth for $d > 0$. Define, for any initial conditions such that $d_0 = d(0) > 0$, the Lyapunov function candidate $\mathcal{L}_\eta$ by

$$\mathcal{L}_\eta = \frac{m}{2d_\infty}\dot{d}^2 + k_I \left[\frac{d}{d_\infty}\left(\ln\left(\frac{d}{d_\infty}\right) - 1\right) + 1\right] \geq 0 \tag{12}$$

Differentiating $\mathcal{L}_\eta$ and recalling equation (11), it yields

$$\dot{\mathcal{L}}_\eta = -k_P \frac{\dot{d}^2}{dd_\infty} \tag{13}$$

This implies that $\mathcal{L}_\eta < \mathcal{L}_\eta(0)$ as long as $d(t) > 0$. Two different cases may occur depending on the initial value of

[1]The optical flow can be computed using a range of algorithms (correlation-based technique, features-based approaches, differential techniques, etc) [1].

$\mathcal{L}$: $\mathcal{L}_\eta(0) < k_I$ and $\mathcal{L}_\eta(0) \geq k_I$. From the expression of the Lyapunov function (12), the first case ($\mathcal{L}_\eta(0) < k_I$) implies that there exists $\varepsilon > 0$ such that $d(t) > \varepsilon > 0,\ \forall t$. Consequently, d remains strictly positive and equation (11) is well defined for all time. Application of LaSalle's principle shows that the invariant set is contained in the set defined by $\dot{\mathcal{L}}_\eta = 0$. This implies that $\dot{d} \equiv 0$ in the invariant set. Recalling (11), it is straightforward to show that d converges asymptotically to d_∞.

For the second situation ($\mathcal{L}_\eta(0) \geq k_I$), we have to show that $d \neq 0$ for all time. Assume that there exists a first time t_1 such that $\dot{d}(t_1) < 0$ and $0 < d(t_1) < d_\infty$. If we show that there exists a second time $t_2 > t_1$ such that $\dot{d}(t_2) = 0$ and $d(t_2) > 0$ then, $\mathcal{L}_\eta(t_2) < k_I$ and conditions of the first case are verified. Therefore, $d > 0$ for all time $t > t_2$ and consequently $d > 0$ for all time $t > 0$. We proceed using a proof by contradiction. Assume that for all time $t > t_1$, $\dot{d}(t) < 0$. This implies $d(t) < d(t_1) < d_\infty,\ \forall t > t_1$. Thus, recalling equation (11), it follows that there exists $\varepsilon > 0$ such that $\ddot{d}(t) > \varepsilon > 0,\ \forall t > t_1$. As a consequence, there exists a time $T > t_1$ such that d converges to 0 ($d \geq 0$) when t tends to T. Recalling equation (11), it yields:

$$\ddot{d} > -\frac{k_P}{m}\frac{\dot{d}}{d} > 0,\ \forall t > t_1 \tag{14}$$

Integrating this equation, it follows:

$$\dot{d} - \dot{d}(t_1) > -\frac{k_P}{m}\ln\left(\frac{d}{d(t_1)}\right),\ \forall t > t_1 \tag{15}$$

Since d converges to 0, $\dot{d}$ converges to $+\infty$. This contradicts the fact that $\dot{d} < 0, \forall t > t_1$ and consequently $d(t) > 0, \forall t$ and converges to d_∞.

Proof of part 2: Let $v^\parallel$ be the planar velocity $\pi_\eta v \in \mathcal{I}$. Recall the control law in equation (8) in the plane normal to η:

$$u^\parallel = \pi_\eta u = k_P\frac{v^\parallel}{d} + k_I\int_0^t \frac{v^\parallel}{d}\,d\tau + mg\pi_\eta e_3 \tag{16}$$

Recall the dynamics of the component of (5) in this plane:

$$m\dot{v}^\parallel = -k_P\frac{v^\parallel}{d} - k_I\int_0^t \frac{v^\parallel}{d}\,d\tau + \Delta^\parallel \tag{17}$$

where $\Delta^\parallel = \pi_\eta\Delta$. Let δ_1 be the following variable:

$$\delta_1 = \int_0^t \frac{v^\parallel}{d}\,d\tau - \frac{\Delta^\parallel}{k_I} \tag{18}$$

Differentiating δ_1, it yields:

$$\dot{\delta}_1 = \frac{v^\parallel}{d} \tag{19}$$

Consider the following Lyapunov function candidate:

$$\mathcal{L}_{\pi_\eta} = k_I\frac{\|\delta_1\|^2}{2} + m\frac{\|\delta_2\|^2}{2} \tag{20}$$

where $\delta_2 = v^\parallel/\sqrt{d}$. Differentiating $\mathcal{L}_{\pi_\eta}$ and recalling equation (17), one obtains:

$$\dot{\mathcal{L}}_{\pi_\eta} = -\|\delta_2\|^2\frac{\left(k_P + m\dot{d}/2\right)}{d} \tag{21}$$

Using the fact that $(d, \dot{d})$ converges to $(d_\infty, 0)$, one can insure that there exists a time T and $\varepsilon > 0$ such that

$$\frac{(k_P + m\dot{d}/2)}{d} > \varepsilon > 0,\ \forall t > T$$

This implies that $\mathcal{L}_{\pi_\eta}(t) < \mathcal{L}_{\pi_\eta}(T),\ \forall t > T$. Application of LaSalle's principle shows that the invariant set is contained in the set defined by $\dot{\mathcal{L}}_{\pi_\eta} = 0$. This implies that $\delta_2 \equiv 0$ in the invariant set and therefore $v^\parallel$ converges asymptotically to 0. Moreover, recalling (17), it is straightforward to show that δ_1 converges to 0.

Finally, using the fact that $v = v^\perp\eta + v^\parallel$, it follows that v converges to zero. ■

IV. Landing control

In this section we consider the landing manoeuvre of the aerial robot on a horizontal plane moving vertically. The primary goal is to address the question of the vertical landing on a moving platform (target) with unknown dynamics. The most important application concerns landing on a deck of a ship in high seas and tough weather [16], [18], [21], [22]. A common model of the vertical motion z_G of the platform as the motion of the ship involved by the sea waves is [16]:

$$z_G = \sum_{i=1}^{n} a_i\cos\left(\omega_i t + \phi_i\right) \tag{22}$$

where $a_i,\ \omega_i,\ \phi_i$ are unknown constants. The classical approach estimates the parameters of motion and uses these to add a feed-forward compensation term in the control input. In this paper, we consider a more general vertical motion z_G of the platform with respect to the inertial frame $\mathcal{I}$. We assume that z_G is a smooth function of class $\mathcal{C}^2$ (z_G and $\dot{z}_G$ are continuous functions of time t) such that $\ddot{z}_G$ is bounded by a known value.

We also assume that the target plane belongs to the plane x-y of the inertial frame so that $d \equiv h$ is the height of the vehicle with respect to the moving platform. Thus, unlike the previous section (III), the relative velocity of the vehicle with respect to the target is $(v - \dot{z}_G e_3)$. Consequently, it is straightforward to verify that (7) becomes (see [8] and [9]):

$$w = \frac{v - \dot{z}_G e_3}{h} + noise$$

and,

$$w_z = \langle w, e_3\rangle = -\frac{\dot{h}}{h} + noise \tag{23}$$

Define

$$w^d = (0, 0, \omega^*)^T,\ \ \omega^* > 0,$$

as the desired average optical flow. Note that the vertical component of the inertial average optical flow acts analogously to optical flow divergence. It is straightforward to show that when $w = w^d$ one has $(v_x, v_y) = (0, 0)$ and $v_z = h_0\omega^*\exp(-\omega^* t)$ along with $h = h_0\exp(-\omega^* t)$ insuring a smooth vertical landing.

Therefore, previous control law (8) for the x-y dynamics may be used to stabilise the flight over the landing pad. We

still need to provide the control scheme for the remaining degree of freedom ($h \equiv |z - z_G|$). In particular, we consider the desired set point, ω^*, for the flow divergence (the flow in the normal direction to the target plane) and look for a control law that achieves regulation of $(\dot{h}/h + \omega^*)$. The controller is a direct application of the controller proposed in [17], along with a complete and more rigorous proof of the exponential convergence and stability of the couple $(h, \dot{h})$ to $(0, 0)$ despite unknown dynamics and unknown terms:

$$m\dot{v} = -u + mge_3 + \Delta(t) \tag{24}$$

Theorem 4.1: Consider the dynamics of the vertical component of (24) and assume that the vertical component u_z of the thrust vector of u is the control input. Choose u_z as

$$u_z = mk(w_z - \omega^*) + mg \tag{25}$$

Assume that z_G is at least $\mathcal{C}^2$ and that $\ddot{z}_G$ and Δ are bounded. Choose the control gain k such that:

$$k > \frac{|\Delta_z|_{\max} + m|\ddot{z}_G|_{\max}}{m\omega^*} \tag{26}$$

Then, for all initial conditions such that $h_0 > 0$ ($h_0 \equiv |z(0) - z_G(0)|$), $h(t) > 0$ remains positive and converges exponentially to zero.

Proof: Since the dynamics of the considered system are decoupled, recall the dynamics of the third component of (24):

$$m\dot{v}_z = -u_z + mg + \Delta_z \tag{27}$$

It follows that the height dynamics can be written:

$$m\ddot{h} = mk(w_z - \omega^*) - \Delta_z + m\ddot{z}_G \tag{28}$$

$$= -mk\left(\frac{\dot{h}}{h} + \alpha(t)\right) \tag{29}$$

where,

$$\alpha(t) = \left(\omega^* + \frac{\Delta_z}{mk} - \frac{\ddot{z}_G}{k}\right)$$

Recalling condition (26), it is straightforward to show that $\alpha(t)$ is a bounded positive function ($\alpha(t) > 0,\ \forall t > 0$). The dynamics (29) are well defined as long as $h(t) > 0$, hence there exists a first time $T_{\max}$, possibly infinite, such that $(h, \dot{h})$ is well defined on $[0, T_{\max})$. Define the following virtual state on $[0, T_{\max})$:

$$\zeta(t) = h(t)\exp\left(\frac{\dot{h}}{k}\right) \tag{30}$$

Differentiating ζ and recalling equations (29), it yields

$$\dot{\zeta} = -\alpha(t)\zeta \tag{31}$$

Since $\zeta_0 = h_0$, it follows that on $[0, T_{\max})$

$$h_0 \exp\left(-\alpha_{\max} t\right) < \zeta(t) < h_0 \exp\left(-\alpha_{\min} t\right)$$

It remains to show that $\dot{h}$ is bounded to ensure, using (30), that there exist $\epsilon_1, \epsilon_2 > 0$ such that

$$\epsilon_1 h_0 \exp\left(-\left|\alpha\right|_{\max} t\right) < h(t) < \epsilon_2 h_0 \exp\left(-\left|\alpha\right|_{\min} t\right)$$

for all time $t \in [0, T_{\max})$. We will show that $T_{\max} = \infty$ using continuity. This will ensure that $(h, \dot{h})$ is well defined on $[0, \infty)$, and $h(t)$ converges exponentially to 0.

To do this, we first prove that the sign of $\dot{h}(t)$ does not change more than once. Two situations may occur:

- $\dot{h}(0) \geq 0$: to show that there exists a time T on $[0, T_{\max})$ such that $\dot{h}(T) < 0$, assume the converse; that is, $\dot{h} \geq 0$ for all time t. Thus, by exploiting (30),

  $$\zeta(t) \geq h_0$$

  Since ζ is exponentially decreasing, it follows that $\dot{\zeta} < -\alpha_{\min}\zeta$. Therefore, there exists a time T such that $\zeta(T) < h_0$. This contradicts the assumption.
- $\dot{h}(0) < 0$: to show that $\dot{h} < 0$ for all time, assume the converse; that is, there exists T such that $\dot{h}(T) = 0$ and $\dot{h}(t) < 0,\ \forall t < T$. Since $\dot{h}$ is continuous and recalling (29), it follows that there exists $\delta > 0$ and $\epsilon > 0$ such that $\ddot{h}(t) < -\epsilon,\ \forall t \in [T - \delta, T]$. Recalling (30), it yields:

  $$\zeta(t) < h(t),\ \forall t \in [T - \delta, T]$$

  Moreover, since $\dot{h}(T) = 0$,

  $$\zeta(T) = h(T)$$

  Hence the contradiction.

To show that $\dot{h}$ is lower bounded, let $\mathcal{J}$ be the following storage function:

$$\mathcal{J} = \frac{1}{2}\dot{h}^2 \tag{32}$$

Differentiating $\mathcal{J}$ and recalling equations (29), it yields:

$$\dot{\mathcal{J}} = -k\frac{\dot{h}}{h}\left(\dot{h} + \alpha h\right) \tag{33}$$

It follows that $\mathcal{J}$ is negative as long as $|\dot{h}| > \alpha h$. Since there exists a time T such that $\dot{h} < 0,\ \forall t > T$, it follows that $h > 0$ is upper bounded. Consequently, $\dot{h}$ is bounded. Therefore, since ζ is exponentially decreasing, one can ensure that h remains positive and exponentially decreasing on $[T, T_{\max})$.

Now, we prove that $T_{\max} = \infty$ and thus that ζ is well defined on $[0, \infty)$. If $T_{\max} \neq \infty$, there exists a positive number δ such that $h(t) > 0$ (by continuity) and such that $\dot{h}$ is unbounded on $[T_{\max}, T_{\max} + \delta)$. This contradicts the above discussion. It follows that h converges exponentially to 0. Moreover, using (32) and (33) with direct application of the Input-to-State-Stable (ISS) argument, it follows that $\dot{h}$ is exponentially stable. ■

Remark 4.2: Note that the stability of the control law (8) used for the lateral dynamics can be proved in the case where $\Delta^{\parallel}$ is constant or slowly varying ($\dot{\Delta}^{\parallel}(t) \approx 0$); the proof is similar to the second part of the proof of Theorem 3.1 using the fact that $\dot{h}$ is bounded and converges to 0. △

V. SIMULATIONS

In order to evaluate the efficiency of the proposed servo control technique, a simulation of the vertical motion of the idealised quadrotor dynamics (27) is presented. The simulation considers only the vertical landing problem of the vehicle on a moving platform. The mass of the vehicle is chosen $m = 0.85$kg; it is the mass identified for the physical system used for experimentation. The control gain is set to $k = 10$, the error Δ_z is chosen $\Delta_z = -0.9$. The vertical motion of the platform is chosen as follows:

$$z_G = a_G \sin(2\pi f_G t) \text{ with } a_G = 0.1m \text{ and } f_G = 0.3s^{-1}$$

The desired set point ω^* is set to 0.5s^{-1}. Using the above values of the different parameters involved in the vertical motion (29), it is straightforward to show that condition (26) is verified.

Figures 1 show the closed-loop trajectory of the vertical motion of the vehicle. We verify that the vertical optical flow w_z remains positive for all time even if it does not reach ω^* and the height $h = -z + z_G$ converges exponentially to 0 despite the fact that the vertical motion of the platform is unknown. Note that the trajectory in red on the figure corresponds to the desired trajectory.

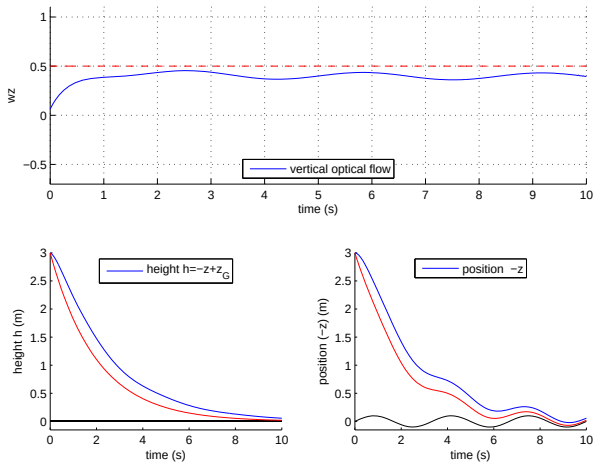

Fig. 1: Simulation of vertical landing using controller (25)

VI. EXPERIMENTAL RESULTS

In this section, experimental results of the above algorithms designed for the full dynamics of the system are presented. The UAV used for the experimentation is the X4-flyer (a quad-rotor) made by the CEA (Fig. 2a), described in the reference [9].

The considered target plane is a large board and textures are made of random contrasts (Fig. 2b). The camera embedded is looking directly down. A Pyramidal implementation of the Lucas-Kanade [13] algorithm is used to compute the optical flow. The efficiency of the algorithm is increased by defocusing the camera to low-pass filter images. The field of view of the aperture is of $30°$ around the direction of observation $\eta = e_3$. Optical flow is computed on 210 points on this aperture and a least-square estimation of motion parameters is used to obtain robust measurements of the average optical flow w [24]. Given that the divergent flow is

(a) The X4-flyer UAV

(b) Hovering flight above the landing pad

Fig. 2

relatively low compared to the lateral flow in the front and back directions [5] and since only the divergent flow is used for landing manoeuvre, the control approach is split into two sequential phases. The first one concerns the hovering flight; it is performed to insure that the lateral flow is regulated to zero and then the vertical landing manoeuvre is applied in a second step. During the experiments, the yaw velocity is regulated to zero. It has no effect on the proposed control scheme. The drone is teleoperated near the target, so that textures are visible. The landing pad is moving laterally and vertically to show performances of the control algorithms. Estimation of the UAV's relative position is computed from the optical flow as follows:

$$\frac{\tilde{\xi} - \tilde{\xi}_0}{h_0} = \int_0^t w\gamma(\tau)\, d\tau = \int_0^t w \exp\left(-\int_0^\tau w_z\, d\delta\right) d\tau \tag{34}$$

Where $\tilde{\xi}$ denotes the relative position of the UAV with respect to the platform: $\tilde{\xi} = \xi - \xi_G$. Note that

$$\gamma(\tau) = \exp\left(-\int_0^\tau w_z\, d\delta\right) = \exp\left(\int_0^\tau \frac{\dot{h}}{h}\, d\delta\right) = \frac{h(\tau)}{h_0} \tag{35}$$

For the vertical landing, the desired set point w^d is set to $(0, 0, 0.1)^T$, this ensures a relatively rapid descent (approximatively in 10s).

Figures 3 show the result using controller (8) for the stabilisation of the X4-flyer with respect to the platform (from 0s to 140s) and controller (25) for the vertical landing manoeuvre (from 140s). For the stabilisation phase, the platform is moving laterally (from 0s to 100s) and vertically (from 100s to 140s). During the landing manoeuvre ($t \geq 140$s) the platform is moving only vertically. Figures 3 show the exponential convergence of the height with a good behaviour while the lateral position remains stable. Note that the relative position $(y - y_G)$ converges around -1, this is due to an initial bias of the inertial measurements in y-direction that

has been compensated by the integral term of the controller. Note also that, contrary to what was expected, the height h is slowly oscillating during the landing phase. This implies that condition (26) is not verified for all time t and therefore, the positivity of $\alpha(t)$ (see Section IV) is not always guaranteed. This problem is mainly due to the fact that experimental constraints (large time latency, outer loop's sampling time which is of 15Hz) prevent us from choosing a higher gain k which strictly respect the condition. Note also that, due to the landing gear, the final position is not $h \equiv 0$.
This result can be watched on the video accompanying the paper.

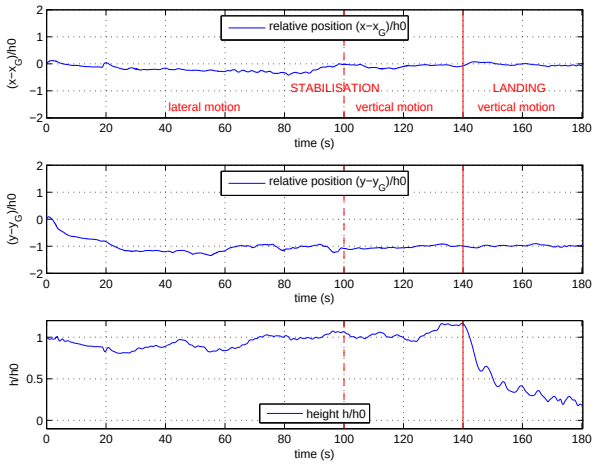

Fig. 3: Vertical landing on a moving platform

VII. Concluding remarks

This paper presented a rigorous nonlinear controller for vertical landing of a VTOL UAV using the measurement of average optical flow on a spherical camera along with the IMU data. Different controllers corresponding to different control objectives (stabilisation and vertical landing) of the VTOL UAV with respect to a moving platform have been proposed and the stability of the closed-loop systems has been analysed. Experimental results have been presented to show the performance of the approach considered.

VIII. Acknowledgments

This work was partially funded by Naviflow grant and by ANR project SCUAV (ANR-06-ROBO-0007) and by the Australian Research Council through the ARC Discovery Project DP0880509, "Image based teleoperation of semi-autonomous robotic vehicles".

References

[1] J. L. Barron, D. J. Fleet, and S. S. Beauchemin. Performance of optical flow techniques. *International Journal of Computer Vision*, 12(1):43–77, 1994.

[2] Geoffrey L. Barrows, Javaan S. Chahl, and Mandyam V. Srinivasan. Biomimetic visual sensing and flight control. In *Seventeenth International Unmanned Air Vehicle Systems Conference*, Bristol, UK, April 2002.

[3] S. Bertrand, T. Hamel, and H. Piet-Lahanier. Stability analysis of an uav controller using singular perturbation theory. In *Proceedings of the 17th IFAC World Congress*, Seoul, Korea, July 2008.

[4] Antoine Beyeler, Jean-Christophe Zufferey, and Dario Floreano. Vision-based control of near-obstacle flight. *Autonomous Robots*, 27(3):201–219, 2009.

[5] J. S. Chahl, M. V. Srinivasan, and S. W. Zhang. Landing strategies in honeybees and applications to uninhabited airborne vehicles. *The International Journal of Robotics Research*, 23(2):101–110, 2004.

[6] Matthew A. Garratt and Javaan S. Chahl. Vision-based terrain following for an unmanned rotorcraft. *Journal of Field Robotics*, 25:284–301, 2008.

[7] William E. Green and Paul Y. Oh. Optic flow based collision avoidance. *IEEE Robotics & Automation Magazine*, 15(1):96–103, 2008.

[8] T. Hamel and R. Mahony. Visual servoing of an under-actuated dynamic rigid-body system: An image based approach. *IEEE Transactions on Robotics and Automation*, 18(2):187–198, April 2002.

[9] B. Herisse, F-X. Russotto, T. Hamel, and R. Mahony. Hovering flight and vertical landing control of a vtol unmanned aerial vehicle using optical flow. In *IEEE/RSJ Int. Conf. on Intelligent Robots and Systems*, Nice, France, September 2008.

[10] J. Sean Humbert, R. M. Murray, and M. H. Dickinson. Pitch-altitude control and terrain following based on bio-inspired visuomotor convergence. In *AIAA Conference on Guidance, Navigation and Control*, San Francisco, CA, 2005.

[11] H. K. Khalil. *Nonlinear Systems*. Prentice Hall, New Jersey, U.S.A., second edition, 1996.

[12] J. Koenderink and A. van Doorn. Facts on optic flow. *Biol. Cybern.*, 56:247–254, 1987.

[13] B. Lucas and T. Kanade. An iterative image registration technique with an application to stereo vision. In *Proceedings of the Seventh International Joint Conference on Artificial Intelligence*, pages 674–679, Vancouver, 1981.

[14] R. Mahony, P. Corke, and T. Hamel. Dynamic image-based visual servo control using centroid and optic flow features. *Journal of Dynamic Systems Measurement and Control*, 130(1), 2008.

[15] R. Mahony and T. Hamel. Robust trajectory tracking for a scale model autonomous helicopter. *International Journal of Non-linear and Robust Control*, 14:1035–1059, 2004.

[16] L. Marconi, A. Isidori, and A. Serrani. Autonomous vertical landing on an oscillating platform: an internal-model based approach. *Automatica*, 38:21 –32, 2002.

[17] C. McCarthy, N. Barnes, and R. Mahony. A robust docking strategy for a mobile robot using flow field divergence. *IEEE Transactions on Robotics*, 24(4):832 – 842, 2008.

[18] So-Ryeok Oh, Kaustubh Pathak, Sunil K. Agrawal, Hemanshu Roy Pota, and Matt Garratt. Approaches for a tether-guided landing of an autonomous helicopter. *IEEE Transactions on Robotics*, 22(3):536 – 544, 2006.

[19] F. Ruffier and N. Franceschini. Visually guided micro-aerial vehicle: automatic take off, terrain following, landing and wind reaction. In *Proceedings of international conference on robotics and automation*, LA, New Orleans, April 2004.

[20] F Ruffier and N. Franceschini. Optic flow regulation: the key to aircraft automatic guidance. *Robotics and Autonomous Systems*, 50:177–194, 2005.

[21] Srikanth Saripalli, James F. Montgomery, and Gaurav S. Sukhatme. Visually-guided landing of an unmanned aerial vehicle. *IEEE transactions on robotics and automation*, 19(3):371 – 380, 2003.

[22] Cory S. Sharp, Omid Shakernia, and S. Shankar Sastry. A vision system for landing an unmanned aerial vehicle. In *IEEE International Conference on Robotics and Automation*, 2001.

[23] M.V. Srinivasan, S.W. Zhang, J. S. Chahl, E. Barth, and S. Venkatesh. How honeybees make grazing landings on flat surfaces. *Biological Cybernetics*, 83:171183, 2000.

[24] S. Umeyama. Least-squares estimation of transformation parameters between two point patterns. *IEEE Trans. PAMI*, 13(4):376–380, 1991.

[25] K. P. Valavanis. *Advances in Unmanned Aerial Vehicles*. Springer, 2007.

[26] Xilin Yang, Hemanshu Pota, Matt Garratt, and Valery Ugrinovskii. Prediction of vertical motions for landing operations of uavs. In *Proceedings of the 47th IEEE Conference on Decision and Control*, Cancun, Mexico, December 2008.